5

Performance Analysis of Magnetic Resonant System Based on Electrical Circuit Theory

Hisayoshi Sugiyama
Dept. of Physical Electronics and Informatics
Osaka City University
Japan

1. Introduction

In this chapter, performances of wireless resonant energy links(Karalis et al., 2008) based on nonradiative magnetic field(Kurs et al., 2007) generated by a pair of coils are analyzed using electrical circuit theory. (from now on, this type of energy link is simply called as *magnetic resonant system*.) Based on the analyses, several aspects of the magnetic resonant systems concerning their power transmission characteristics become clear. In addition, optimal design parameters of the system are obtained that maximize the power transmission efficiency or effective power supply.

Simple and common processes based on the electrical circuit theory, other than specialized ones such that coupled-mode theory(Haus, 1984) or antenna theory(Stutzman, 2011), are applied to the analyses throughout this chapter. Therefore, intuitive and integrated comprehension of the magnetic resonant systems may be possible especially in the comparison of principle with the conventional electromagnetic induction systems as described in the next section.

In section 2, the difference of principle of magnetic resonant systems from that of conventional electromagnetic induction systems is explained where the role of magnetic resonance become clear when the coils are located apart. In section 3, based on the difference from the conventional systems, the inherent characteristics of power transmission of magnetic resonant systems are explained focusing on the resonance current in coils that affects the efficiency of the power transmission. In section 4, based on the power transmission characteristics of magnetic resonant systems, optimal system designs are investigated that maximize the power transmission efficiency or effective power supply under constraints of coil sizes and voltages of power sources. Finally, section 5 summarizes these discussions.

2. Electromagnetic induction system and magnetic resonant system

In this section, first, the principle of conventional electromagnetic induction systems is explained based on the electrical circuit theory. In comparison with this principle of the conventional systems, second, that of magnetic resonant systems is explained where the role of magnetic resonance become clear in power transmission between distant coils.

2.1 Electromagnetic induction system

An electromagnetic induction system is commonly used as a voltage converter that consists of closely coupled pair of coils with different numbers of wire turns. In this system, alternating voltage applied to one part of coil induces a different terminal voltage of the counterpart at the same frequency. Because mutual inductance of coils is so large by the proximity of them even with iron core that constrains the magnetic flux within their inner field, the adequate high power transmission efficiency is obtained by this conventional system.

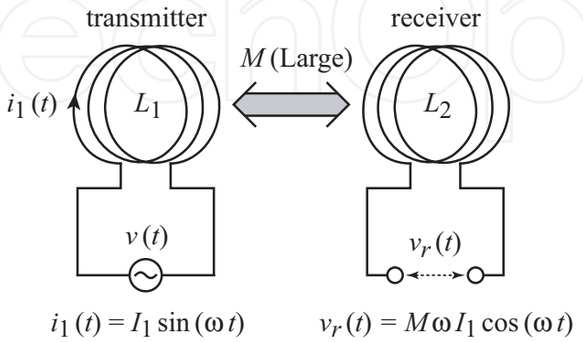

Fig. 1. Electromagnetic induction system.

Figure 1 shows a simple model of the electromagnetic induction system consisting of a pair of coils with different inductances L_1 and L_2. They are closely coupled and have large mutual inductance M. No load resistance is connected to the receiver coil. In this system, the transmitter coil is driven by a voltage source $v(t)$ and current $i_1(t) = I_1 \sin(\omega t)$ flows through its wire at some stationary state of the system. Almost of the alternating magnetic flux generated by this current interlinks the receiver coil. This flux linkage Φ is derived by $i_1(t)$ and the mutual inductance M of coils as $\Phi = Mi_1(t)$. Because the differential of the flux linkage Φ equals the induced voltage of the coil, appears at the terminal of the receiver coil.

$$\begin{aligned} v_r(t) &= \frac{d}{d\,t}\,\Phi \\ &= M\,\frac{d\,i_1(t)}{d\,t} \\ &= M\,\omega\,I_1\,\cos(\omega t) \end{aligned} \tag{1}$$

In electromagnetic induction systems, the receiver terminal voltage $v_r(t)$ becomes so large that enough power transmission is possible if some load resistance is connected to the terminal to consume properly the transmitted power. This is mainly because the mutual inductance M of coils is so large by the proximity of them and by the iron core that prevents magnetic flux leakage as mentioned above.

Whereas, assuming that the coil pair is set apart, and the magnetic flux generated by the transmitter coil diffuses around it without any spacial constraint, only a fragment of the magnetic flux interlinks the receiver coil and their mutual inductance M becomes small. In this case, only a limited voltage $v_r(t)$ appears at the receiver terminal and insufficient power transmission can be obtained even with the proper load resistance at the terminal.

The magnetic resonant system compensates this problem of small M of the detached coil pair with their magnetic resonance as described in the next subsection.

2.2 Magnetic resonant system

In case that the coil pair is set apart in the electromagnetic induction system shown in Fig. 1, M becomes small and Eq.(1) indicates that the receiver terminal voltage $v_r(t)$ decreases accordingly. However, Eq.(1) also indicates that the decrease of M can be compensated with high frequency ω or large current amplitude I_1 of the transmitter coil.

Commonly, the power supply frequency ω is specified in electromagnetic induction systems used as voltage converters. Whereas, any system that is designed only to transmit power between coils may be driven at an arbitrary high frequency. However, alternating magnetic field at very high frequency possibly generates electromagnetic radiation that dissipates power around the system. This transmission power loss becomes noticeable especially when the distance of coils approaches the wavelength of the electromagnetic radiation.

The magnetic resonant systems utilize the other factor in Eq.(1) that compensates small M between distant coils: transmitter coil current amplitude I_1. This principle is explained by a simple model of a magnetic resonant system shown in Fig. 2 where inductances of coils are set to the same value L for the simplicity and their mutual inductance M is assumed to be small. In this model of the magnetic resonant system, a parallel capacitance C is connected to each coil of the system and therefore a pair of LC-loops are configured that makes the magnetic resonance possible between the loops with huge coil currents[1]. These huge coil currents induced in the magnetic resonance between the LC-loops compensates small M of distant coils providing adequate receiver terminal voltage $v_r(t)$.

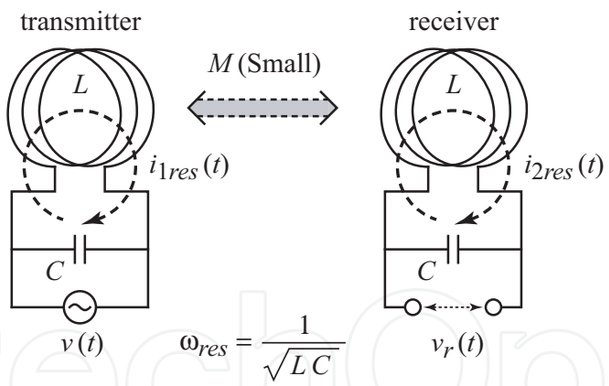

Fig. 2. Magnetic resonance without power transmisson.

The resonance between these LC-loops occurs as follows. First, at some frequency ω, the current $i_1(t)$ of the transmitter coil generates alternating magnetic flux and a segment of this flux interlinks the receiver coil. Second, to decrease this interlinking flux alternation, inverted current $i_2(t)$ begins to flow in the receiver coil and a segment of the inverted flux interlinks the transmitter coil. This negative return of a flux segment decreases the flux alternation inside the transmitter coil mitigating its inductive reactance. Third, because of the decreased

[1] In many of the magnetic resonant systems, such as the experimental system reported in (Kurs et al., 2007), each C is not visible as a condenser but exists as a stray capacitance within the coils.

reactance of the transmitter coil that is driven by the stable voltage source $v(t)$, its coil current $i_1(t)$ increases generating more the magnetic flux and the process returns to the first stage [2].
These stages repeats until the system arrives at some stationary state that depends on the loop impedances of both LC-loops. However, when ω approaches the resonance frequency ω_{res} that equals $1/\sqrt{LC}$, because the loop impedance of each LC-loop becomes zero at this critical point, its loop current grows to huge one $i_{1res}(t)$ at the transmitter, or $i_{2res}(t)$ at the receiver as shown in Fig. 2.
This critical incident, where currents of LC-loop pair diverges synchronously at the resonance frequency ω_{res}, is called *magnetic resonance* because their mutual interference is mediated by alternating magnetic field. When this magnetic resonance occurs in the system shown in Fig. 2, the huge coil currents $i_{1res}(t)$ and $i_{2res}(t)$ generates noticeable terminal voltage $v_r(t)$ that is formulated by:

$$v_r(t) = M\,\frac{d}{dt}i_{1res}(t) \;+\; L\,\frac{d}{dt}i_{2res}(t)\,, \tag{2}$$

or

$$v_r(t) = \frac{1}{C}\int i_{2res}(t)\,dt\,. \tag{3}$$

Moreover, if proper load resistance is connected to the terminal, enough power becomes available that the transmitter supplies in spite of long distance between the coils.
As described above, a magnetic resonant system utilizes magnetic resonance between LC-loops of transmitter and receiver. The role of the magnetic resonance is to utilize huge coil currents that makes the power transmission possible between the loops even though they are located apart. According to Eq.(1), this principle of magnetic resonant system can be explained that the huge coil current $i_1(t)$ compensates the small M to generate a sufficient amplitude of $v_r(t)$.
In the next section, the performance of power transmission of a magnetic resonant system is investigated with a load resistance at the receiver. Other characteristics are also examined including actual resonance frequency ω_{res} and amplitudes of resonance currents $i_{1res}(t)$ and $i_{2res}(t)$.

3. Power transmission by magnetic resonant system

In magnetic resonant systems, voltage source supplies electric power to the LC-loop at the transmitter and load resistance at the receiver extracts this power from the LC-loop of its side. Between the LC-loops, alternating magnetic field carries the power at the resonance frequency where both coil currents diverge synchronously fastening their magnetic coupling.
In this section, power transmission characteristics of a magnetic resonant system with a load resistance is investigated. As the result, examples are shown of actual resonance frequency, resonance currents of coils, and transmitted power in relation with system parameters.

[2] This intuitive description of the system behavior focusing on the inductive reactances of LC-loops is valid when ω exceeds the resonance point of the loops. Because the capacitive reactances become dominant in the loops when ω falls behind the resonance point, $i_1(t)$ and $i_2(t)$ become inphase in this range of ω and the description must be modified accordingly.

3.1 System analysis

Figure 3 shows a magnetic resonant system adopted for the investigation. This system is equivalent to that shown before in Fig. 2 except for the load resistance R of the receiver and notations of currents $i_1(t) \sim i_4(t)$ each for the indicated line in the figure. Magnetic coupling between coils is indicated by mutual inductance M or coupling factor k. k equals M/L and therefore never exceeds unity. The power supplied by the voltage source $v(t)$ (input power) and that consumed by the load resistance R (output power) are denoted by P_{in} and P_{out}, respectively.

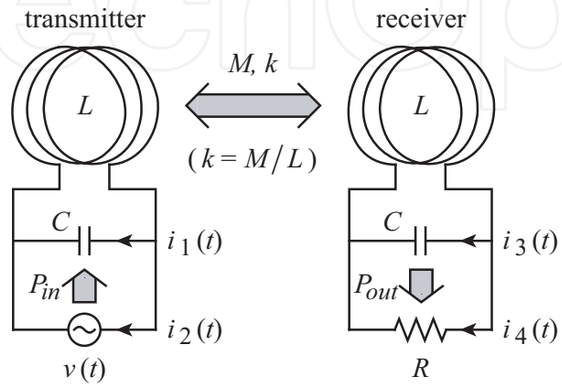

Fig. 3. Power transmission by magnetic resonant system.

Assuming that the system is at some stationary state, the voltage source $v(t)$ is expressed by complex exponential as $V\exp(j\omega t)$ and $i_1(t) \sim i_4(t)$ are expressed as $I_1\exp(j\omega t) \sim I_4\exp(j\omega t)$, respectively. Voltage amplitude V is set to be a real number. Whereas, the amplitudes of currents $I_1 \sim I_4$ may be complex numbers indicating the phase shift of $i_1(t) \sim i_4(t)$ from $v(t)$, respectively.

Among these amplitudes and parameters of the system shown in Fig. 3, simultaneous equations:

$$\begin{cases} V = j\omega\{\, L(I_1 + I_2) \,+\, M(I_3 + I_4)\,\} \\ V = -I_1 \,/\, (j\omega C) \\ 0 = R\, I_4 + j\omega\{\, L(I_3 + I_4) \,+\, M(I_1 + I_2)\,\} \\ R\, I_4 = I_3 \,/\, (j\omega C) \end{cases} \tag{4}$$

are established. Here, the angular frequency ω is assumed to be low enough in relation to the coil distance. Therefore, in the first and third lines of the equations, the interaction between coils by M occurs with no phase difference[3].

The input power P_{in} and output power P_{out} are derived as:

$$P_{in} \,=\, \frac{1}{2}\, V\, \Re(I_2)\,, \;\; P_{out} \,=\, \frac{1}{2}\, R\, |\, I_4\, |^2\,. \tag{5}$$

($\Re(x)$ means the real part of x.) These values must be equal to each other according to energy conservation law. This is because power dissipation caused by electromagnetic radiation or

[3] For example, in the case of $\omega = 2\pi \cdot 1$[MHz] corresponding to the electromagnetic wave length of 300[m], coil distance of 3[m] or less may satisfy this assumption.

other power consumers such as inner resistances of coils are not included in Fig. 3 nor in Eq.(4). This is confirmed by calculating Eq.(5) with I_2 and I_4 derived from Eq.(4). As the result, the equivalent transmission power P is obtained as[4],

$$P = P_{in} = P_{out} = \frac{1}{2} \cdot \frac{V^2 k^2 R}{L^2(1-k^2)^2\omega^2 + \{1 - CL(1-k^2)\omega^2\}^2 R^2}. \tag{6}$$

This expression of power P is valid on the system shown in Fig 3 that is driven at any frequency ω. However, the system becomes magnetic resonant system only at the resonance frequency ω_{res}. In the next subsection, this frequency ω_{res} is examined.

3.2 Resonance frequency

The resonance frequency ω_{res} is derived here assuming that the transmission power P becomes maximum at this critical frequency. According to this assumption, ω_{res} and the maximum power P_{res} is determined as[5]:

$$\omega_{res} = \sqrt{\frac{2CR^2 - L(1-k^2)}{2L(1-k^2)C^2R^2}}. \tag{7}$$

$$P_{res} = \frac{2V\ 2k^2C^2R^3}{L(1-k^2)\left(4CR^2 - L(1-k^2)\right)} \tag{8}$$

Besides these expressions, that are rather complicated and cannot be recognized intuitively, approximated ones $\widetilde{\omega}_{res}$ and $\widetilde{P}_{res}$ are available. First, $\widetilde{\omega}_{res}$ is:

$$\omega_{res} \simeq \widetilde{\omega}_{res} = \frac{1}{\sqrt{LC(1-k^2)}}. \tag{9}$$

This approximation is easily recognized by the equation:

$$\omega_{res} = \widetilde{\omega}_{res} \cdot \sqrt{1 - \frac{\epsilon}{2}}, \quad \epsilon = \frac{1}{RC\,\widetilde{\omega}_{res}}. \tag{10}$$

As explained later, ϵ becomes very small provided the system is designed to perform as a magnetic resonant system. Therefore, in most cases, $\widetilde{\omega}_{res}$ in Eq.(9) approximates well the resonance frequency ω_{res}.

The approximated form $\widetilde{\omega}_{res}$ indicates that the resonance frequency of the system shown in Fig. 3 shifts from the inherent point $1/\sqrt{LC}$ of a LC-loop depending on the coupling factor k of the coil pair. k falls to 0 when the coils are located far away and approaches 1 when they become close to each other. Therefore, the resonance frequency $\widetilde{\omega}_{res}$ increases from the inherent point when the distance of LC-loops are set properly so as to they can perform power transmission.

The variable ϵ in Eq.(10) indicates the degree of how well the RC parallel impedance can be approximated to only resistance R at the frequency $\widetilde{\omega}_{res}$. This RC parallel impedance is connected to the terminal of receiver coil shown in Fig. 3. The variable ϵ equals the ratio of the absolute value of impedance $1/(j\omega C)$ of the capacitance C to the resistance R.

[4] The solutions $I_1 \sim I_4$ of Eq.(4) are written in Appendix A.1.

[5] The derivation process of Eq.(7) and (8) is described in Appendix A.2.

A small ϵ means that the capacitive impedance dominates in the RC parallel impedance and therefore the receiver forms almost pure LC-loop[6]. Because this LC-loop must work as a resonator in magnetic resonant systems, R must be set properly to make ϵ small. Whereas, in case that the resistance R is set small in relation to the capacitive impedance $1/(j\omega C)$, the circuit almost becomes resistance R. In this case, the LC-loop of the receiver scarcely work as a resonator to receive power from the transmitter. Furthermore, when R falls behind a threshold, ω_{res} in Eq.(10) becomes imaginary quantity. In such cases, the magnetic resonance cannot occur. This threshold R_{th} is derived by $\epsilon = 2$ as,

$$R_{th} = \frac{1}{2C\,\widetilde{\omega}_{res}} = \frac{1}{2}\sqrt{\frac{L(1-k^2)}{C}}. \tag{11}$$

This means that if receiver load resistance R adequately exceeds this value R_{th}, the system shown in Fig. 3 performs well as a magnetic resonant system and the approximation $\widetilde{\omega}_{res}$ of the resonance frequency ω_{res} is valid. Whereas, if R is set equal to or less than R_{th}, the system cannot be a magnetic resonant system at any frequency ω.
Finally, the approximated value of the maximum power transmission $\widetilde{P}_{res}$ is derived by substitution of $\widetilde{\omega}_{res}$ (Eq.(9)) into P (Eq.(6)) as:

$$\widetilde{P}_{res} = \frac{V^2k^2CR}{2L(1-k^2)}. \tag{12}$$

3.3 An example of power transmission

Based on the equations derived in the previous subsections, an example of power transmission characteristics of a magnetic resonant system is shown with actual parameters. Besides the coil inductance L, other parameters of coil pair are assumed to be the same. The parameters are set as follows:
Coil radius a, its wire turns N, and its thickness t are set to 5[cm], 20[turns], and 5[mm], respectively. From these values, its self inductance L is calculated to be 97.9[μH][7].
The inherent resonance frequency of the LC-loop is set to 10[KHz]. This value is not the angular frequency but the actual frequency and equals $1/(2\pi\sqrt{LC})$. Because L is already fixed, the capacitance C is derived from this frequency as 2.59[μF].
Eq.(11) indicates that the threshold R_{th} of the load resistance R becomes maximum when k equals 0. This maximum R_{th} is derived from L and C as 3.07[Ω]. As an adequately exceeding value over this R_{th}, the load resistance R of the receiver is set to 500[Ω]. These parameters are listed in Table 1.
With these parameters adopted, the resonance frequency f_{res} of the magnetic resonant system and coupling factor k of its coil pair are calculated and shown in Fig. 4. Horizontal axis represents the distance d between the coils. f_{res} is calculated by Eq.(9). k is calculated from coil parameters and the distance d assuming that coils are confronting each other with the same axis[7]. As this graph shows, both values increase as the distance d of coils decreases. However, the increase of the resonance frequency f_{res} from the inherent value $1/(2\pi\sqrt{LC})$ is not noticeable until d falls behind the diameter 10[cm] of coils.

[6] Notice that a small impedance dominates in parallel circuit because electric current tends to flow the wire with smaller impedance than others.
[7] The calculations of L and k are described in Appendix A.3.

coil parameters	notation	value	unit
inductance	L	97.9	μH
radius	a	5	cm
wire turn	N	20	turn
thickness	t	5	mm
other parameters	notation	value	unit
capacitance	C	2.59	μF
load resistance	R	500	Ω
voltage amplitude	V	100	Volt

Table 1. System parameters.

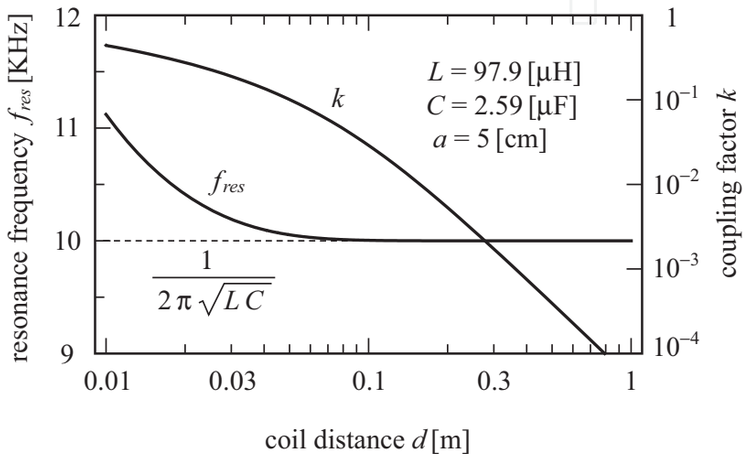

Fig. 4. Resonance frequency f_{res} of the system and coupling factor k of the coil pair.

When the voltage source $v(t)$ in Fig. 3 drives the system at the resonance frequency ω_{res} (or f_{res} shown in Fig. 4), magnetic resonance occurs between its LC-loops with huge loop currents and with power transmission from the transmitter to the receiver. This transmission power P_{res} and loop currents of the magnetic resonant system are calculated and shown in Fig. 5. Horizontal axis represents coil distance d as same as Fig. 4. Vertical axis represents P_{res} and amplitudes $|I_1| \sim |I_4|$ of the electric currents $i_1(t) \sim i_4(t)$, respectively. In addition to the parameters specified above, the amplitude V of the voltage source $v(t)$ is set to 100[V]. P_{res} is calculated by Eq.(12) and amplitudes of the electric currents are calculated by Eq.(A1)∼(A4) in Appendix.
This graph shows several features on this magnetic resonant system as follows:

- The transmitted power P_{res} varies noticeably from about 650[W] to 0.01[W] as the distance d of coils increases from their radius 5[cm] to its ten times long 50[cm].
- Whereas, the amplitudes of resonance loop currents $|I_1|$ and $|I_3|$ do not decrease similarly. Especially, $|I_1|$ keeps almost constant value 16[A] throughout the indicated range of d.
- In comparison with these huge resonance currents, $i_2(t)$ and $i_4(t)$ perform actual power transmission (see Eq.(5)). Concerning the practical distance d of coils over their diameter 10[cm], the amplitudes of these currents $|I_2|$ and $|I_4|$ do not exceed moderate value.

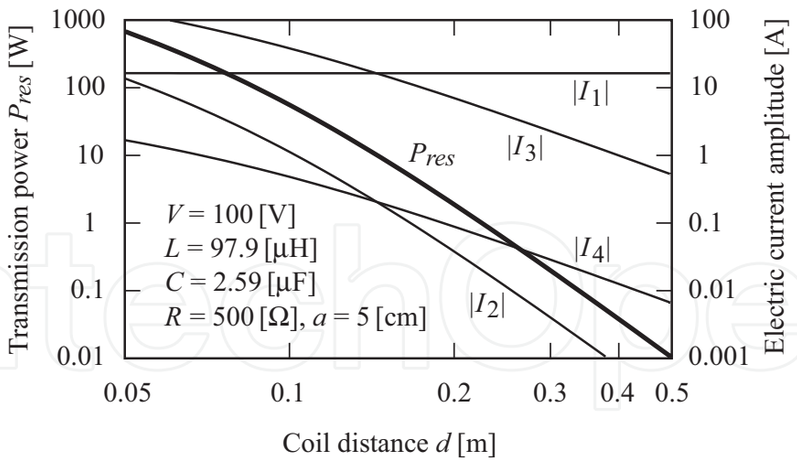

Fig. 5. Transmission power P_{res} and current amplitudes.

The noticeable decrease of transmission power P_{res} along with the increase of coil distance d seems not to be a serious problem according to Eq.(12). This equation indicates that the decrease of P_{res} can be compensated with the square of voltage amplitude V.

On the other hand, huge amplitudes of loop currents $|I_1|$ and $|I_3|$ possibly affect seriously the power transmission efficiency of the system. This is because the inner resistances of coils consume a part of transmission power in proportional to the square of current amplitude $|I_1|$ or $|I_3|$.

In the next section, these power losses caused by inner resistances of coils are taken into account on the analysis of magnetic resonant system performance. As the results, the designs are obtained for the power transmission efficiency maximum or for the effective power supply maximum. In addition, it is found that any combination of the efficiency and power supply is possible provided the system is driven over a critical frequency.

4. Optimal designs of magnetic resonant system with internal resistances of coils

As shown in the previous section, example values of coil currents ($|I_1|$ and $|I_3|$ in Fig. 5) become huge at the resonance point of the system in comparison with other currents ($|I_2|$ and $|I_4|$ in the same figure) that concern actual power transmission.

These huge coil currents may bring noticeable power dissipation caused by internal resistances of coils even though their amounts are insignificant. This is because the Joule loss within a wire of resistance R is proportional to the square of its current flow $i(t)$ as $Ri(t)^2$ and therefore is sensitive to the current amplitude especially when the amplitude is very large.

Therefore, in actual designs of magnetic resonant systems, internal resistances of coils must be taken into account and appropriate system parameters must be determined from the viewpoint of the power transmission performances that may degrade caused by the internal resistances of coils.

In this section, power transmission performances of magnetic resonant systems are investigated taking into account the internal resistances of coils. As the results, appropriate system designs are obtained for the optimal system performances.

4.1 System analysis

Figure 6 shows the magnetic resonant system with the internal resistances of coils adopted for the investigation. The basics of the system is equivalent to that shown in Fig. 3. The differences from this previous system are as follows:

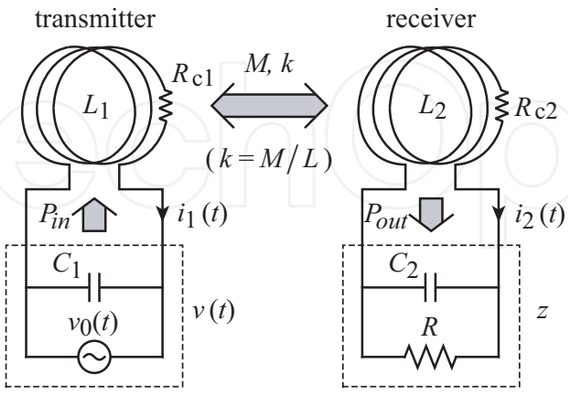

Fig. 6. Magnetic resonant system with internal resistances of coils.

1. For the generality of investigations and system designs, constraint of symmetry between LC-loops of transmitter and receiver is eliminated from their parameters.
2. According to this scheme of generality, coil inductances of transmitter and receiver are set to L_1 and L_2, respectively. (From now on, parameters with suffix '1' means that of transmitter and suffix '2' means that of receiver.) Similarly, capacitances are set to C_1 and C_2.
3. For the evaluation of Joule losses within the coils, the internal resistances R_{c1} and R_{c2} are additionally adopted as shown in Fig. 6.
4. $i_1(t)$ and $i_2(t)$ in Fig. 3 are integrated into unique coil current $i_1(t)$ of the transmitter. Similarly, coil currents of receiver are integrated into $i_2(t)$.

In addition, some elements are substituted by integrated ones as follows for the convenience of the analysis.

1. The part of the transmitter consists of C_1 and the voltage source (denoted by $v_0(t)$) is substituted by a single voltage source $v(t)$ as shown in the left part of Fig. 6. This substitution is possible because the voltage and the frequency with that the transmitter coil is driven is determined by $v_0(t)$ itself. Whereas, C_1 only let the resonance current $i_1(t)$ bypass this voltage source.
2. The part of the receiver consists of C_2 and R is substituted by a complex impedance z as shown in the right part of Fig. 6. This substitution embeds C_2 in z as a component of capacitive reactance.

According to the same assumption as put in the previous section, that the system is at some stationary state, the voltage source $v(t)$ is expressed by $V\exp(j\omega t)$. Similarly, $i_1(t)$ and $i_2(t)$ are expressed by $I_1\exp(j\omega t)$ and $I_2\exp(j\omega t)$, respectively. The amplitudes of currents I_1 and I_2 may be complex numbers indicating the phase shift of $i_1(t)$ and $i_2(t)$ from $v(t)$, respectively. Among these amplitudes and parameters of the system shown in Fig. 6, simultaneous equations:

$$\begin{cases} V = j\omega L_1 I_1 + j\omega M I_2 + R_{c1} I_1 \\ z I_2 + j\omega L_2 I_2 + j\omega M I_1 + R_{c2} I_2 = 0 \end{cases} \tag{13}$$

are established[8]. The power supply P_{in} from $v(t)$, and the power consumption P_{out} of z are given by,

$$P_{in} = \frac{1}{2} V \Re(I_1), \quad P_{out} = \frac{1}{2} \Re(z) \mid I_2 \mid^2. \tag{14}$$

In the previous section, it was confirmed by Eq.(6) that P_{in} equals P_{out}. However, because of internal resistances of coils R_{c1} and R_{c2} that consume a part of P_{in} at the transmitter and that of P_{out} at the receiver, P_{in} and P_{out} become different to each other in the system shown in Fig. 6. Taking into account these power dissipations of Joule losses by R_{c1} and R_{c2}, the relational expression:

$$P_{out} = P_{in} - \frac{1}{2} R_{c1} |I_1|^2 - \frac{1}{2} R_{c2} |I_2|^2 \tag{15}$$

is established[9] (from now on, P_{out} is called as *effective power supply*). Eq.(15) indicates that the power transmission efficiency:

$$\xi = \frac{P_{out}}{P_{in}} \tag{16}$$

exists somewhere below one depending on the system parameters and the resonance frequency that the system is driven at. (from now on, this efficiency ξ is simply called as *transmission efficiency*.)

In the following subsections, first, the internal resistance of a coil is estimated in relation with the coil configuration. Based on this estimation, second, the optimal receiver impedance z is investigated that maximizes the transmission efficiency ξ or effective power supply P_{out} itself. Finally, examples of these optimal designs are shown with actual parameters of magnetic resonant systems.

4.2 Internal resistance of coils

According to Eq.(15), internal resistances R_{c1} and R_{c2} must be reduced enough to obtain admissible transmission efficiency ξ of the magnetic resonant system. An elementary way to reduce the internal resistances is to extend the cross section of wire of the coils. This is because the internal resistance of a wire is inversely proportional to its cross section.

However, unrestrained increase of wire radius causes enlargement of the coil configuration. In many designs of magnetic resonant systems, the dimensional specifications exist that restrict the coil configuration. Because of this reason, in the estimation of internal resistance of a coil, the coil configuration must be specified first, and then the internal resistance of the coil is derived in relation with its wire turns, coil inductance, and maximum wire radius under the restriction of the coil configuration.

[8] As mentioned in the previous section, the angular frequency ω is assumed to be low enough in relation to the coil distance.

[9] When a current $i(t)$ is expressed by $I \exp(j\omega t)$, Joule loss $R\, i(t)^2$ is estimated as $(1/2)R|I|^2$ in average.

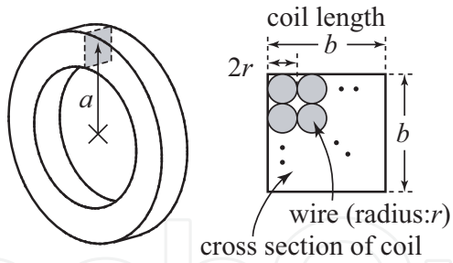

Fig. 7. Coil configuration.

Figure 7 shows the coil configuration adopted to the estimation of the internal resistance. It is assumed that the cross section of coil is square and the wire is wound densely within the cross section. Parameters a, b, and r represent coil radius, coil length, and wire radius, respectively. According to these assumptions and notations, equations:

$$\begin{cases} L = 2 \cdot 10^{-7} \pi^2 K(\eta) a N^2 / \eta \\ R_c = \rho \cdot 2\pi a N / (\pi r^2) \end{cases} \tag{17}$$

are obtained where L and R_c represent coil inductance and its internal resistance, respectively. K, η, N, and ρ are Nagaoka coefficient, configuration index, wire turns, and the resistivity of wire material, respectively[10]. Configuration index η equals $b/2a$ and wire turns N approximately equals $(d/2r)^2$.
From these equations, a simple relation between the coil inductance L and its internal resistance R_c is derived as:

$$R_c = \sigma L, \ \sigma = \frac{10^7}{\pi^2} \cdot \frac{\rho}{a^2 K(\eta)\, \eta} \ . \tag{18}$$

where σ denotes a proportional coefficient between R_c and L and has unit of (1/second)[11]. Because the expression of σ does not include wire parameters N and r, this coefficient is determined only by the coil configuration and the resistivity ρ of wire material.

4.3 Optimal performances of magnetic resonant system

For the optimal performances of magnetic resonant system, two types of receiver impedance z are derived.

1. Optimal impedance z^e that maximizes the transmission efficiency ξ provided other parameters of the system are fixed.
2. Optimal impedance z^p that maximizes the effective power supply P_{out} provided other parameters of the system are fixed.

[10] The second equation of (17) assumes that R_c inversely proportional to the wire cross section (πr^2). However, this simple assumption will not valid when the coil current alternates at high frequency because of the skin effect of wire(Maqnusson, et al.). Therefore, Eq.(17) must additionally assume that the frequency is low enough or the wire is *Litz wire* that reduces the skin effect(Kazimierczuk, 2009).

[11] Considering that ωL and R_c have the same unit (Ω), σ must have the same unit as ω according to Eq.(18).

The process of derivation of z^e and z^p is as follows. First, I_1 and I_2 are derived from Eq.(13). Second, the effective power supply P_{out} and the transmission efficiency ξ are derived from Eq.(14) and (16), respectively. Third, z^e and the maximum transmission efficiency ξ_m are derived along with z^p and the maximum effective power supply P_m (from now on, simply called as *maximum power*). Finally, according to Eq.(18), equations $R_{c1} = \sigma_1 L_1$ and $R_{c2} = \sigma_2 L_2$ are applied to these results for the elimination of internal parameters[12].
The derived formulas are as follows. First, the maximum transmission efficiency ξ_m, the real part z_r^e and the imaginary part z_i^e of z^e are

$$\xi_m = 1 - 2\frac{\sqrt{\sigma_1\sigma_2}\sqrt{\sigma_1\sigma_2 + k^2\omega^2} - \sigma_1\sigma_2}{k^2\omega^2} \tag{19}$$

$$z_r^e = L_2\sqrt{\sigma_2^2 + \frac{k^2\sigma_2\omega^2}{\sigma_1}},\ z_i^e = -L_2\,\omega \tag{20}$$

Obviously, transmission efficiency does not depend on the voltage source amplitude V. This is confirmed by (19). In addition, this formula is independent also of inductances L_1 and L_2. These coil parameters are hidden in σ_1 and σ_2 that specifies the coil configurations.
Second, the maximum power P_m, the real part z_r^p and the imaginary part z_i^p of z^p are

$$P_m = \frac{V^2k^2\omega^2}{8L_1\left(\sigma_1^2\sigma_2 + k^2\sigma_1\omega^2 + \sigma_2\omega^2\right)} \tag{21}$$

$$z_r^p = L_2\frac{\sigma_1^2\sigma_2 + (\sigma_1k^2 + \sigma_2)\,\omega^2}{\sigma_1^2 + \omega^2},\ z_i^p = -L_2\,\omega\frac{\sigma_1^2 + (1-k^2)\,\omega^2}{\sigma_1^2 + \omega^2} \tag{22}$$

In contrast to Eq.(19), Eq.(21) includes V and L_1. However, as the essential value of maximum power, normalized maximum power $\widehat{P_m}$ is derived independently of V and L as:

$$\widehat{P_m} = (L_1/V^2)P_m = \frac{k^2\omega^2}{8\left(\sigma_1^2\sigma_2 + (\sigma_1k^2 + \sigma_2)\omega^2\right)} \tag{23}$$

This normalized maximum power $\widehat{P_m}$ has unit of (second)[13] and is utilized in the process of optimal system designs for the maximum transmission efficiency described in the next subsection.

4.4 Examples of optimal system design

According to the formulas derived in the previous subsection, the system design procedure for the optimal performance of magnetic resonant systems is shown with actual design examples. Though the previous analyses can be applied to the cases where transmitter and receiver coils are not symmetrical, they are assumed to be symmetrical in the followings. The symmetrical coil pair is essential in a power supply link between mobile robots that configure power supply network of multi-robot systems(Sugiyama, 2009; 2010; 2011). Because of this reason, coil inductances and their internal resistances are substituted by the same variable L and R_c, respectively.

[12] The details of this process are described in the Appendix A.4∼A.7.
[13] According to Eq.(23), and considering that k has no unit, the unit of $\widehat{P_m}$ is the same as (ω^2/σ^3) and is equal to $(1/\sigma)$.

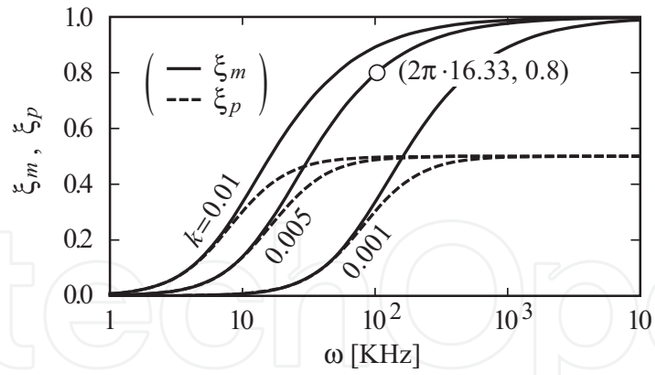

Fig. 8. Maximum transmission efficiency ξ_m when $z = z^e$ and transmission efficiency ξ_p when $z = z^p$.

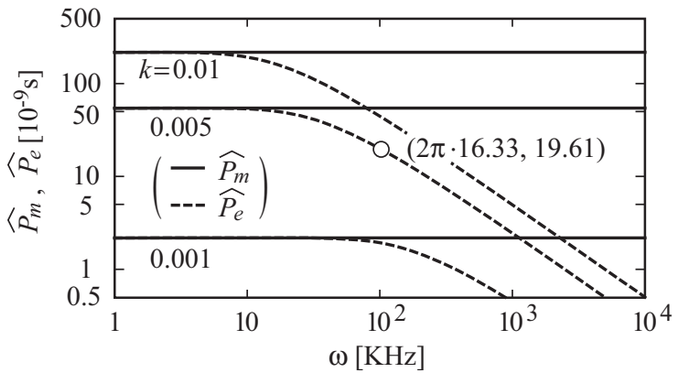

Fig. 9. Normalized maximum power $\widehat{P_m}$ when $z = z^p$ and normalized power $\widehat{P}_e$ when $z = z^e$.

Figure 8 indicates the maximum transmission efficiency ξ_m versus frequency ω by solid lines calculated by Eq.(19). Dashed lines indicate the transmission efficiency ξ_p when the impedance is set as z^p that maximizes effective power supply.
On the other hand, Fig. 9 indicates the normalized maximum power $\widehat{P_m}$ versus frequency ω by solid lines calculated by Eq.(23). Dashed lines indicate the normalized power $\widehat{P}_e$ that is derived by multiplying P_e by (L/V^2) similarly to $\widehat{P_m}$. Where, P_e equals effective power supply P_{out} when the receiver impedance is set as z^e that maximizes transmission efficiency. ξ_p and $\widehat{P}_e$ are expressed as follows:

$$\xi_p = \frac{k^2\omega^2}{2\left(2\sigma^2 + k^2\omega^2\right)} \tag{24}$$

$$\widehat{P}_e = \left(L_1/V^2\right) P_e = \frac{k^2\omega^2\sqrt{\sigma^2 + k^2\omega^2}}{2\left(\sigma^2 + \omega^2 + k^2\omega^2\right)\left(2\sigma^2 + k^2\omega^2 + 2\sigma\sqrt{\sigma^2 + k^2\omega^2}\right)} \tag{25}$$

In both figures, three values of coupling factor k between coils are applied as indicated. Other parameters are as follows:
The wire material of coils is assumed to be copper. Therefore, its resistivity ρ is set to $1.72 \cdot 10^{-8}[\Omega\,\mathrm{m}]$. The coil radius a and its configuration index η are set to 5[cm] and 0.3, respectively.

Applying these values to Eq.(18), the proportional coefficient σ between R_c and L is calculated to be 57.37[1/s]. These parameters are listed in Table 2 [14].

coil parameters	notation	value	unit
wire resistivity	ρ	$1.72 \cdot 10^{-8}$	Ωm
radius	a	5	cm
configuration index	η	0.3	-
proportional coefficient	σ	57.37	1/s

Table 2. System parameters.

Figure 8 shows two points. First, when the coupling factor k is fixed according to the relative position of the coils, the minimum frequency ω_{min} exists, which satisfies the target value ξ_{target} of the transmission efficiency. Second, when the impedance z^p is adopted for maximum power supply, ξ_p cannot exceed 50% even if the frequency ω increases enough. Therefore, in the practical designs where ξ_{target} exceeds 50%, z^p cannot be applied as the receiver impedance.
On the other hand, Fig. 9 shows that when $z = z^p$, the normalized maximum power $\widehat{P_m}$ stays nearly constant, whereas when $z = z^e$, the normalized power $\widehat{P}_e$ decreases as ω increases. However, because the normalized value $\widehat{P}_e$ is derived from P_e multiplied by (L/V^2) as shown by Eq.(25), any amount of power supply is possible by adjusting this coefficient.
From these results, a design procedure of a magnetic resonant system for the maximum transmission efficiency is derived as follows.

1. Specify these items:
   - System parameters except for the receiver impedance z.
   - Target transmission efficiency ξ_{target} that exceeds 50%.
   - Target effective power supply P_{target}.
2. According to system parameters except for z, and to ξ_{target}, the minimum frequency ω_{min} is determined.
3. To make minimum the power dissipation by electromagnetic radiation, the frequency ω of the voltage source $v_0(t)$ must be as low as possible. Because of this reason, ω is fixed to the minimum frequency ω_{min}.
4. At this frequency ω_{min}, the value of normalized power $\widehat{P}_e$ is determined. Then, (V^2/L) is derived from $P_{target}/\widehat{P}_e$.
5. Under the constraint that (V^2/L) is fixed, voltage source amplitude V and coil inductance L can be set arbitrary. However, in many cases L may be set first because it affects receiver impedance z^e.
6. The optimal receiver impedance z^e is determined by Eq.(20) that makes the magnetic resonant system satisfy the target efficiency ξ_{target} and target effective power supply P_{target} at the minimum frequency ω_{min}.

According to this design procedure, a design example is described as follows:

[14] At these parameters, the minimum value 0.001 of k corresponds to the coil distance of 44.7[cm] (the relationship between $k(= M/L)$ and the coil distance d is described in Appendix A.3). On the other hand, the maximum value 10^7[Hz] of the indicated range of ω corresponds to the wavelength of 190[m]. Therefore, the assumption put on Eq.(13) may be valid over these figures.

1. System parameters are specified by Table 2. In addition, coupling factor k of coils is set to 0.005 (the distance d between them is 25.5[cm][15]). ξ_{target} is set to 80% and P_{target} is set to 10[W].
2. ω_{min} is found to be $2\pi \cdot 16.33$[KHz] from Fig. 8 (a white dot indicates this point).
3. $\widehat{P}_e$ is found to be 19.61×10^{-9}[s] from Fig. 9 (a white dot indicates this point).
4. P_{target} (10[W]) is obtained when $(V^2/L) = 5.100 \times 10^8$. Under this constraint, L and V are fixed to 0.3331[mH] and 412.2[V], respectively[16].
5. According to Eq.(20), z^e is obtained as $0.1720 - j34.18$. This impedance corresponds to $R = 6.795$[KΩ] and $C = 0.2850$[μF] for RC-parallel impedance as shown in Fig. 6.

Besides this design example of magnetic resonant system, more general design specifications are indicated in Fig. 10 and 11 with extended range of system parameters.
Figure 10 indicates voltage source amplitude V by solid lines and its minimum frequency f_{min} by dashed lines. Whereas Fig. 11 indicates receiver load resistance R by solid lines and LC-loop capacitance C by dashed lines.
In both figures, system parameters and target power supply P_{target} are the same as the previous system design. Coupling factor k of coils is set to three different values: 0.001, 0.005, 0.01 as shown in the figure. These values correspond to 44.7, 25.5, and 19.8[cm] of coil distance d, respectively. Horizontal axis represents ξ_{target} that exceeds 0.5.

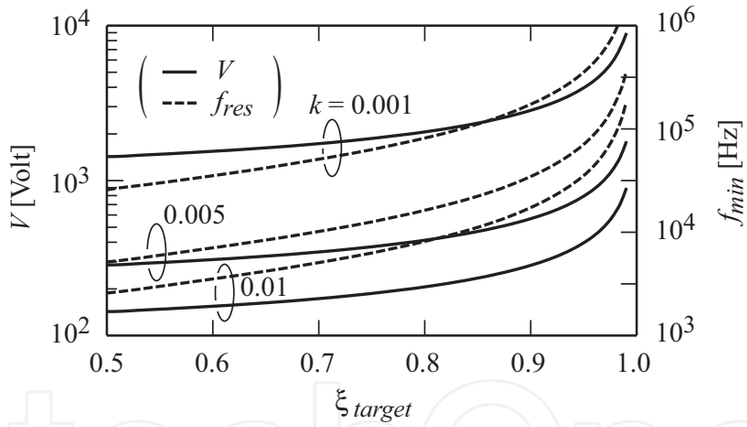

Fig. 10. Voltage source amplitude V and minimum frequency f_{min}.

Fig. 10 shows the difficulty of system design when coils are set apart. For example, when k equals 0.001, this corresponds to 44.7[cm] of coil distance d as mentioned above, voltage source amplitude V exceeds 1000[V] at 0.7 of ξ_{target}. This impractical voltage amplitude may be reduced by adjusting L under the constraint of (V^2/L) is fixed. However, because L affects the optimal receiver impedance z^e concerning actual configuration of RC parallel impedance, reasonable value of L must be investigated further in relation with the whole system design.
The influence of L to the RC parallel impedance can be recognized in Fig. 11. When ξ_{target} increases in Fig. 10, the frequency f_{min} increases especially at high ξ_{target}. This means that the inherent resonance frequency $1/\sqrt{LC}$ increases accordingly at high ξ_{target}. However,

[15] d can be inversely derived from k by Eq.(A9) and $k = L/M$.
[16] This value of L is derived from Eq.(17) substituting 50 for the wire turn N.

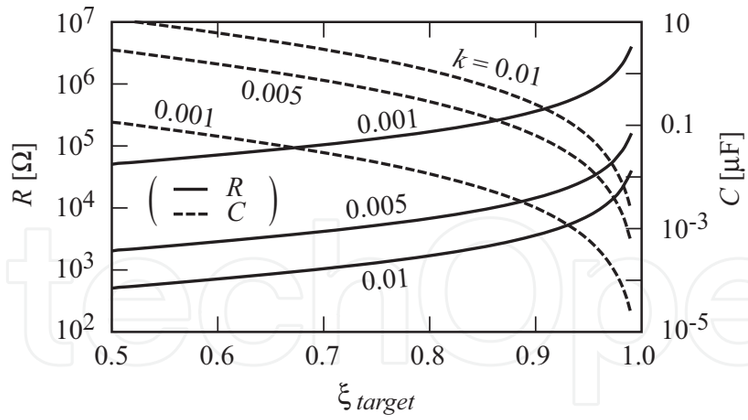

Fig. 11. Receiver load resistance R and LC-loop capacitance C.

because L is fixed to the constant value in this case, C must decrease excessively as shown in Fig. 11. This small value of C constrains R to increase enough to keep its domination in RC parallel impedance and to keep the receiver approximately pure LC-loop as discussed before in subsection 3.2. Because of this reason, the values of R and C alternate excessively when ξ_{target} is high. Adjustment of L to some reasonable value will alleviate this excessive alternation of the system parameters.

5. Conclusion

Performances of wireless resonant energy links based on nonradiative magnetic field generated by a pair of coils (magnetic resonant system) are analyzed using electrical circuit theory.

First, the difference of principle of magnetic resonant systems from that of conventional electromagnetic induction systems is explained. As the result, it became clear that the role of magnetic resonance is to keep the magnetic coupling between coils that are located apart by compensating their small mutual inductance with huge coil currents.

Second, based on the difference from the conventional systems, the inherent characteristics of power transmission of magnetic resonant systems are explained including the expressions of resonance frequency and power transmission at the resonance frequency. In addition, examples of huge resonance currents are indicated that may degrade power transmission efficiency with internal resistances of coils.

Finally, taking into account the internal resistances of coils, optimal system designs are investigated that maximize the power transmission efficiency or effective power supply under constraints of coil sizes and voltages of power sources. As the result, the minimum resonance frequency is determined where the magnetic resonant system satisfies both of target transmission efficiency and target power supply provided the receiver impedance is set properly.

In further studies, these results must be confirmed by comparisons with ones derived from experimental systems. The comparison with experimental results by MIT(Kurs et al., 2007) is already reported(Sugiyama, 2009) where the possibility is shown that the transmission efficiency of the experimental system can be improved with the optimal designs derived in Section 4. In addition, characteristics of an experimental system with symmetrical coil pair is reported(Sugiyama, 2011) that confirms the theoretical results. However, characteristics of

actual magnetic resonant systems with more general designs such as asymmetrical coil pair must be examined to confirm the theoretical results.

6. Appendix[17]

A.1 Expressions of current amplitudes in Fig. 3

$$I_1 = -jVC\omega \tag{A1}$$

$$I_2 = \frac{k^2RV}{(1-k^2)^2L^2\omega^2 + \left(R - C\,(1-k^2)LR\omega^2\right)^2}$$

$$+j\,\frac{V\left(1-C(1-k^2)L\omega^2\right)\left(R^2\left(CL\omega^2\left(2-C(1-k^2)L\omega^2\right)-1\right)-(1-k^2)L^2\omega^2\right)}{L\omega\left((1-k^2)^2L^2\omega^2+\left(R-C(1-k^2)LR\omega^2\right)^2\right)} \tag{A2}$$

$$I_3 = \frac{-Ck(1-k^2)LRV\omega^2}{(1-k^2)^2L^2\omega^2 + (R-C(1-k^2)LR\omega^2)^2}$$

$$-j\,\frac{CkR^2V\omega\left(1-C(1-k^2)L\omega^2\right)}{(1-k^2)^2L^2\omega^2 + \left(R-C(1-k^2)LR\omega^2\right)^2} \tag{A3}$$

$$I_4 = \frac{kRV\left(C(1-k^2)L\omega^2-1\right)}{(1-k^2)^2L^2\omega^2 + \left(R-C(1-k^2)LR\omega^2\right)^2}$$

$$+j\,\frac{k(1-k^2)LV\omega}{(1-k^2)^2L^2\,\omega^2 + \left(R-C(1-k^2)LR\omega^2\right)^2} \tag{A4}$$

A.2 Derivation of Eq.(7) and (8)

First, transform the Eq.(6) into:

$$P = \frac{1}{\alpha+\beta\chi+\gamma\chi^2}\,. \tag{A5}$$

$$\begin{pmatrix} \chi = \omega^2 \\ \alpha = \dfrac{2R}{V^2k^2} \\ \beta = \dfrac{2L(1-k^2)\left\{L(1-k^2)-2CR^2\right\}}{V^2k^2R^2} \\ \gamma = \dfrac{2L^2C^2R^2(1-k^2)^2(1+k^2)^2}{V^2k^2} \end{pmatrix}$$

At the maximum point of P, the differential of Eq.(A5) by χ equals zero. Therefore,

[17] Many of the expressions below are derived in assistance with Mathematica 6.0.

$$\frac{d}{d\chi} P = -\frac{\beta + 2\gamma\chi}{(\alpha + \beta\chi + \gamma\chi^2)^2} = 0$$

$$\chi = \omega^2 = \frac{-\beta}{2\gamma} = \frac{2CR^2 - L(1-k^2)}{2L(1-k^2)C^2R^2} \tag{A6}$$

Eq.(7) equals the square root of Eq.(A6). Eq.(8) is derived by substitution of (7) into (6).

A.3 Derivation of self inductance L and coupling factor k

The self inductance L of a coil is calculated by the equation:

$$L = 2\pi \cdot 10^{-7} \cdot K\,(\,r\,N^2\,/\,\eta\,)\,, \tag{A7}$$

where, η equals (t/a) and K means Nagaoka coefficient(Hayt, 1989).
The coupling factor k equals M/L. Generally, the mutual inductance M of coils C1 and C2 is calculated by:

$$M = 10^{-7} \oint_{c1} \oint_{c2} \frac{d\mathbf{s}_1 \cdot d\mathbf{s}_2}{|\,\mathbf{r}_1 - \mathbf{r}_2\,|} \tag{A8}$$

where, $c1$, $\mathbf{r}_1$, and $\mathbf{s}_1$ means the contour integral of coil C1, a vector from the origin of coordinates to a point on C1, and a tangent vector at the point, respectively. Variables with suffix 2 means that of coil C2(Hayt, 1989).
Especially, when the coils have the same radius a and wire turns N, and when they confronting each other with the same axis, a reduced form is available as:

$$M = 4\pi 10^{-7} a N^2 \int_0^{\pi} \frac{\cos\theta}{\sqrt{2(1-\cos\theta) + (d/a)^2}}\, d\theta\,. \tag{A9}$$

A.4 Expressions of current amplitudes in Fig. 6

$$I_{1r} = \left[V \left(L_1 L_2 k^2 (r_2 + z_r)\omega^2 + r_1 \left((r_2 + z_r)^2 + (z_i + L_2\omega)^2 \right) \right) \right] \Big/ D \tag{A10}$$

$$I_{1i} = \left[-V L_1 \omega \left((r_2 + z_r)^2 + (z_i + L_2\omega) \left(z_i + (1-k^2) L_2 \omega \right) \right) \right] \Big/ D \tag{A11}$$

$$I_{2r} = \left[-V \sqrt{L_1 L_2}\, k\omega (L_1 (r_2 + z_r)\omega + r_1 (z_i + L_2\omega)) \right] \Big/ D \tag{A12}$$

$$I_{2i} = \left[-V \sqrt{L_1 L_2}\, k\omega \left(r_1 (r_2 + z_r) + L_1 \omega \left(-z_i - (1-k^2) L_2 \omega \right) \right) \right] \Big/ D \tag{A13}$$

$$\begin{aligned} D = {} & 2L_1 L_2 k^2 r_1 (r_2 + z_r)\omega^2 + r_1^2 \left((r_2 + z_r)^2 + (z_i + L_2\omega)^2 \right) \\ & + L_1^2 \omega^2 \left((r_2 + z_r)^2 + \left(z_i + (1-k^2) L_2 \omega \right)^2 \right) \end{aligned} \tag{A14}$$

A.5 Expressions of transmission efficiency ξ and effective power supply P_{out}

$$\xi = L_1 L_2 k^2 z_r \omega^2 \Big/ D_1 \tag{A15}$$

$$\begin{aligned} D_1 &= L_1 L_2 k^2 (R_{c2} + z_r)\omega^2 \\ &+ R_{c1}\left((R_{c2}+z_r)^2 + (z_i + L_2\omega)^2\right) \end{aligned} \tag{A16}$$

$$P_{out} = 0.5\, V^2 L_1 L_2 k^2 z_r \omega^2 \Big/ D_2 \tag{A17}$$

$$\begin{aligned} D_2 &= 2L_1 L_2 k^2 R_{c1}(R_{c2}+z_r)\omega^2 \\ &+ R_{c1}^2\left((R_{c2}+z_r)^2 + (z_i + L_2\omega)^2\right) \\ &+ L_1^2\omega^2\left((R_{c2}+z_r)^2 + \left(z_i - \left(-1+k^2\right)L_2\omega\right)^2\right) \end{aligned} \tag{A18}$$

A.6 Derivation of Eq.(19) and (20)

Eq.(A15) does not include z_i and the denominator Eq.(A16) becomes minimum when $z_i = -L\omega$. Therefore, z_i^e is determined independently of z_r^e as:

$$z_i^e = -L_2\,\omega\,. \tag{A19}$$

The transmission efficiency ξ_{opti} at this z_i^e becomes:

$$\xi_{opti} = \xi\,|_{z_i = z_i^e} = \frac{z_r}{Az_r^2 + Bz_r + C}\,. \tag{A20}$$

$$\left(\begin{array}{l} A = \dfrac{R_{c1}}{L_1 L_2 k^2 \omega^2} \\ B = 1 + \dfrac{2R_{c1}R_{c2}}{L_1 L_2 k^2 \omega^2} \\ C = R_{c2} + \dfrac{R_{c1}R_{c2}^2}{L_1 L_2 k^2 \omega^2} \end{array}\right)$$

At the maximum point of above (A20), z_r satisfies $(d\,\xi_{opti}/d\,z_r) = 0$. Therefore,

$$\frac{d\,\xi_{opti}}{d\,z_r} = \frac{-Az_r^2 + C}{(Az_r^2 + Bz_r + C)^2} = 0$$

$$z_r^e = \sqrt{C/A} = \sqrt{R_{c2}\left(R_{c2} + \frac{L_1 L_2 k^2 \omega^2}{R_{c1}}\right)}\,. \tag{A21}$$

This z_r^e gives the maximum ξ_m. Therefore,

$$\xi_m = \xi_{opti}\Big|_{z_r=z_r^e} = \xi\,|_{z_i=z_i^e,\, z_r=z_r^e}$$

$$= 1 - 2\,\frac{\sqrt{R_{c1}R_{c2}}\sqrt{R_{c1}R_{c2} + L_1L_2k^2\omega^2} - R_{c1}R_{c2}}{L_1L_2k^2\omega^2}\ . \tag{A22}$$

Eq.(19) is derived by assigning $R_{c1} = \sigma_1 L_1$, $R_{c2} = \sigma_2 L_2$ to the above (A22) and by some arrangement. Eq.(20) is derived from (A21) and (A19).

A.7 Derivation of Eq.(21) and (22)

The derivation processes of Eq.(21) and (22) are similar to that of Eq.(19) and (20). First, the denominator (A18) of P_{out} (A17) is arranged with coefficients U, V, and W that do not include z_i. Then,

$$D_2 = U + V\,(z_i + W)^2 \tag{A23}$$

$$\left(\begin{array}{l} U = \dfrac{2\left(R_{c1}^2(R_{c2}+z_r) + L_1\left(L_2k^2R_{c1} + L_1(R_{c2}+z_r)\right)\omega^2\right)^2}{R_{c1}^2 + L_1^2\omega^2} \\ V = 2\left(R_{c1}^2 + L_1^2\omega^2\right) \\ W = L_2\,\omega\,\dfrac{R_{c1}^2 + L_1^2(1-k^2)\omega^2}{R_{c1}^2 + L_1^2\omega^2} \end{array}\right)$$

is given. Therefore,

$$z_i^p = -W = -L_2\,\omega\,\frac{R_{c1}^2 + L_1^2(1-k^2)\omega^2}{R_{c1}^2 + L_1^2\omega^2} \tag{A24}$$

is derived. The effective power supply P_{opti} at this z_i^p is arranged with X, Y, and Z that do not include z_r. Then,

$$P_{opti} = P_{out}\,|_{z_i=z_i^p} = \frac{z_r}{Xz_r^2 + Yz_r + Z} \tag{A25}$$

$$\left(\begin{array}{l} X = \dfrac{4R_{c1}^2R_{c2} + 4L_1\left(L_2k^2R_{c1} + L_1R_{c2}\right)\omega^2}{V^2L_1L_2k^2\omega^2} \\ Y = \dfrac{4R_{c1}^2R_{c2} + 4L_1\left(L_2k^2R_{c1} + L_1R_{c2}\right)\omega^2}{V^2L_1L_2k^2\omega^2} \\ Z = \dfrac{2\left(R_{c1}^2R_{c2} + L_1\left(L_2k^2R_{c1} + L_1R_{c2}\right)\omega^2\right)^2}{V^2L_1L_2k^2\omega^2\left(R_{c1}^2 + L_1^2\omega^2\right)} \end{array}\right)$$

is given. Therefore,

$$\frac{d\,P_{opti}}{d\,z_r} = \frac{-Xz_r^2 + Z}{(Xz_r^2 + Yz_r + Z)^2} = 0$$

$$z_r^p = \sqrt{Z/X} = \frac{R_{c1}^2 R_{c2} + L_1\left(L_2 k^2 R_{c1} + L_1 R_{c2}\right)\omega^2}{R_{c1}^2 + L_1^2\omega^2} \tag{A26}$$

is derived. This z_r^p gives the maximum P_m. Therefore,

$$P_m = P_{opti}\Big|_{z_r = z_r^p} = P_{out}\,|_{z_i = z_i^p,\, z_r = z_r^p}$$

$$= \frac{V^2 L_1 L_2 k^2 \omega^2}{8\left(R_{c1}^2 R_{c2} + L_1\left(L_2 k^2 R_{c1} + L_1 R_{c2}\right)\omega^2\right)}\ . \tag{A27}$$

(21) is derived by assigning $R_{c1} = \sigma_1 L_1$, $R_{c2} = \sigma_2 L_2$ to the above (A27) and by some arrangement. (22) is derived from (A26) and (A24).

7. References

H. A. Haus (1984). *Waves and Fields in Optoelectronics*, Prentice-Hall, New Jersey

W. H. Hayt, Jr. (1989). *Engineering Electromagnetics*, McGraw-Hill

A. Karalis; J. D. Joannopoulos & M. Soljacic (2008). Efficient Wireless Non-Radiative Mid-Range Energy Transfer, *Annals of Physics*, Vol. 323, No. 1, pp. 34-48

M. K. Kazimierczuk (2009). *High-Frequency Magnetic Components*, John Wiley & Sons Ltd

A. Kurs; et al. (2007). Wireless Power Transfer via Strongly Coupled Magnetic Resonances, *Science Express*, Vol. 317, No. 5834, pp. 83-86

P. C. Maqnusson, et al. (2000). *Transmission Lines and Wave Propagation, Fourth Edition*, CRC Press

W. L. Stutzman (2011). *Antenna Theory and Design*, John Wiley & Sons Ltd

H. Sugiyama, Optimal Designs for Wireless Energy Link Based on Nonradiative Magnetic Field, *Proceedings of 13th IEEE Int. Symp. on Consumer Electronics*, Kyoto, Japan, May, 2009

H. Sugiyama, Autonomous Chain Network Formation by Multi-Robot Rescue System with Ad Hoc Networking, *Proceedings of IEEE Int. Workshop on Safety, Security, and Rescue Robotics*, Bremen, Germany, July 2010

H. Sugiyama, Optimal Designs for Wireless Energy Link with Symmetrical Coil Pair, *Proceedings of IEEE Int. Microwave Workshop Series on Innovative Wireless Transmission*, Kyoto, Japan, May 2011

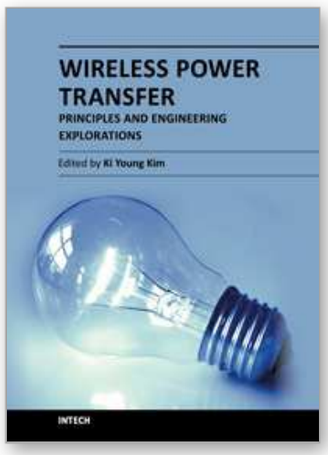

Wireless Power Transfer - Principles and Engineering Explorations
Edited by Dr. Ki Young Kim

ISBN 978-953-307-874-8
Hard cover, 272 pages
Publisher InTech
Published online 25, January, 2012
Published in print edition January, 2012

The title of this book, Wireless Power Transfer: Principles and Engineering Explorations, encompasses theory and engineering technology, which are of interest for diverse classes of wireless power transfer. This book is a collection of contemporary research and developments in the area of wireless power transfer technology. It consists of 13 chapters that focus on interesting topics of wireless power links, and several system issues in which analytical methodologies, numerical simulation techniques, measurement techniques and methods, and applicable examples are investigated.

How to reference
In order to correctly reference this scholarly work, feel free to copy and paste the following:

Hisayoshi Sugiyama (2012). Performance Analysis of Magnetic Resonant System Based on Electrical Circuit Theory, Wireless Power Transfer - Principles and Engineering Explorations, Dr. Ki Young Kim (Ed.), ISBN: 978-953-307-874-8, InTech, Available from: http://www.intechopen.com/books/wireless-power-transfer-principles-and-engineering-explorations/performance-analysis-of-magnetic-resonant-system-based-on-electrical-circuit-theory

INTECH
open science | open minds

InTech Europe
University Campus STeP Ri
Slavka Krautzeka 83/A
51000 Rijeka, Croatia
Phone: +385 (51) 770 447
Fax: +385 (51) 686 166
www.intechopen.com

InTech China
Unit 405, Office Block, Hotel Equatorial Shanghai
No.65, Yan An Road (West), Shanghai, 200040, China
中国上海市延安西路65号上海国际贵都大饭店办公楼405单元
Phone: +86-21-62489820
Fax: +86-21-62489821

IntechOpen